

# Strongly modulated transmissions in gapped armchair graphene nanoribbons with sidearm or on-site gate voltage

H. Tong and M. W. Wu\*

*Hefei National Laboratory for Physical Sciences at Microscale and Department of Physics,  
University of Science and Technology of China, Hefei, Anhui, 230026, China*

(Dated: October 24, 2018)

We propose two schemes of field-effect transistor based on gapped armchair graphene nanoribbons connected to metal leads, by introducing sidearms or on-site gate voltages. We make use of the band gap to reach excellent switch-off character. By introducing one sidearm or on-site gate to the graphene nanoribbon, conduction peaks appear inside the gap regime. By further applying two sidearms or on-site gates, these peaks are broadened to conduction plateaus with a wide energy window, thanks to the resonance from the dual structure. The position of the conduction windows inside the gap can be fully controlled by the length of the sidearms or the on-site gate voltages, which allows “on” and “off” operations for a specific energy window inside the gap regime. The high robustness of both the switch-off character and the conduction windows is demonstrated and shows the feasibility of the proposed dual structures for real applications.

PACS numbers: 72.80.Vp, 73.63.-b, 73.22.Pr

## I. INTRODUCTION

Ever since the monolayer graphene was first successfully produced experimentally,<sup>1</sup> intriguing properties from its strictly two-dimensional structure and massless Dirac-like behavior of low-energy excitation have been intensively investigated.<sup>2,3</sup> Of particular interest are the graphene nanoribbons (GNRs) that are strips of graphene obtained by different methods, e.g., high-resolution lithography,<sup>4,5</sup> chemical means,<sup>6,7</sup> or most recently the unzipping of carbon nanotubes.<sup>8,9</sup> Their semiconducting character with a tunable band gap sensitive to the structural size and geometry makes them good candidates for future electric and spintronic devices.<sup>10</sup> GNRs are classified into two basic groups, namely, armchair and zigzag ones, according to edge termination types.<sup>11–13</sup> In the framework of the nearest neighbor tight binding model, the zigzag GNRs are always metallic and exhibit special spin-polarized edge states.<sup>11–13</sup> For the armchair GNRs with width  $M$  (as defined in Fig. 1), they are metallic when  $M = 3n + 2$ , with  $n$  being an integer, and semiconducting otherwise.<sup>12,13</sup> Graphene field-effect transistors have been experimentally realized by making use of the band gap introduced in GNRs.<sup>6,14</sup> However, large switching voltage up to several volts is needed due to the thick back-gate oxides used in these devices. Moreover, the excellent feature of a tunable band gap in GNRs has not been used in the overall back-gate configuration.<sup>6,14</sup> The electronic transport in GNR-based nanodevices has also been investigated theoretically.<sup>15–18</sup> Particular energy dependences of conductance, resulting from the interference effects, are reported in metallic GNRs<sup>15,16</sup> or in semiconducting ones out of the gap regime.<sup>16,18</sup> However, the robustness of these transport properties against disorder has been shown to be questionable.<sup>15,18–21</sup>

In this work, we introduce two classes of structures

based on gapped armchair GNRs by using either sidearm or on-site gate voltage, which allow “on” and “off” operations in the gap regime. A schematic view of the armchair GNR with one sidearm is shown in Fig. 1. Other configurations, i.e., with two sidearms, one or two on-site gate voltages, are shown together with the numerical results of transport behaviors in the following figures. Such structures are within the reach of nowadays technology, i.e., the patterned GNR can be obtained through high-resolution lithography<sup>4,5</sup> and the contact<sup>4,5</sup> and top-gate<sup>22</sup> technologies are also well developed. It is noted that throughout this work, the width of the GNR is taken as  $M = 21$ , so there is a band gap in the pristine GNR.<sup>12,13</sup> Here the corresponding band gap is about 400 meV. The two terminals of the GNR are connected to semi-infinite metal leads,<sup>16,23,24</sup> which simulates the real experimental condition.<sup>25</sup> Such a configuration is crucial to access possible states in the gap regime of the GNR, due to the propagation modes in the metal leads which are otherwise absent in graphitic ones.<sup>23,24</sup> Meanwhile, the effective length of the sidearm can be electrically adjusted by a gate voltage (not shown in the figure).<sup>26</sup> We show that by increasing the length of the sidearm  $N_s$ , or by increasing the strength of positive or negative on-site gate voltage in the configuration shown in Fig. 4(a), conduction peaks are introduced into the originally switched-off gap regime. The positions of these conduction peaks are determined by the gate voltage, which, in addition to the common property of switching on and off, allows us to selectively choose electrons of a particular energy while filter out the others. We further propose two schemes of structures with markedly improved robustness against disorder by employing two sidearms or on-site gates [see Fig. 5(a) and (d)]. Due to the resonance between the two conduction peaks induced by the dual structure, a conduction plateau, i.e., a broad energy window in which the transmission is close to one, is formed. This conduction

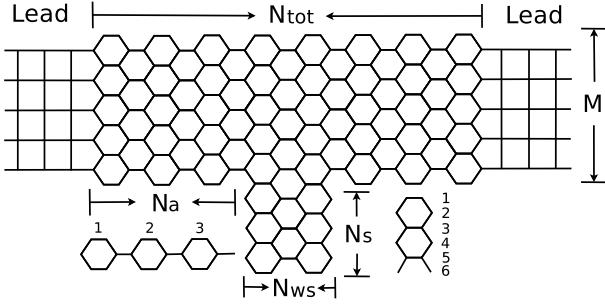


FIG. 1: Schematic view of the armchair GNR with zigzag edged sidearm and metal leads. The insets show how the width and length of the specific structures are defined. Throughout this work, the width of armchair GNR is taken to be  $M = 21$ .

window is very robust against disorder, which makes our proposal highly feasible for real applications.

## II. MODEL AND HAMILTONIAN

We describe the structures consisting of an armchair GNR coupled with metal leads by using the tight-binding Hamiltonian with the nearest-neighbor approximation,

$$H = H_L + H_C + H_R + H_T, \quad (1)$$

where  $H_{L,R}$  are the Hamiltonians of the left and right leads, respectively,  $H_C$  is the Hamiltonian of the GNR and  $H_T$  stands for the coupling between the GNR and the leads. These terms are written as

$$H_\alpha = -t_\alpha \sum_{\langle i_\alpha, j_\alpha \rangle} c_{i_\alpha}^\dagger c_{j_\alpha}, \quad \alpha = L, R \quad (2)$$

$$H_C = \sum_{i_c} \varepsilon_{i_c} c_{i_c}^\dagger c_{i_c} - t \sum_{\langle i_c, j_c \rangle} c_{i_c}^\dagger c_{j_c}, \quad (3)$$

$$H_T = -t_T \sum_{\alpha=L,R} \sum_{\langle i_\alpha, j_c \rangle} (c_{i_\alpha}^\dagger c_{j_c} + H.c.). \quad (4)$$

Here, the index  $i_c$  ( $i_\alpha$ ) is the site coordinate in the GNR (metal leads) and  $\langle i, j \rangle$  denotes pair of nearest neighbors.  $t_\alpha$  and  $t_T$  are hopping parameters in the metal leads and between the leads and the GNR, respectively, which are taken to be equal to the hopping element  $t$  in the GNR.<sup>16,27</sup> The on-site energy in the GNR  $\varepsilon_{i_c}$  is modulated by the on-site gate voltage, which equals  $U_g$  in the gated region and zero elsewhere.

Within the Landauer-Büttiker framework,<sup>28</sup> the transmission amplitude is given by

$$T(E) = \text{tr}[\Gamma_L(E) G_C^r(E) \Gamma_R(E) G_C^a(E)] \quad (5)$$

in which  $\Gamma_{L/R}$  denotes the self-energy of the isolated ideal leads and  $G_C^{r/a}(E)$  represents the retarded/advanced Green's function for the GNR.<sup>29</sup> Here,  $E$  is the Fermi energy in the leads.

## III. RESULTS AND DISCUSSION

### A. Electronic transport in GNRs with one sidearm or on-site gate voltage

We first investigate the transport properties in the GNR with one sidearm as shown in Fig. 1. In Fig. 2(a)-(c), the transmissions are plotted as function of the Fermi energy. The transmission in the pristine GNR is indicated by the red solid curve in Fig. 2(a). It is seen that the band gap manifests itself in the electronic transport behavior that the transmission is well below  $10^{-3}$  in the gap regime, i.e.,  $E_F \in (-200, 200)$  meV. This may serve as the “off” state of the device with excellent switch-off character. By increasing the length of the sidearm  $N_s$  with fixed width  $N_{ws} = 10$ , one notices that two conduction peaks from the positive and negative energy sides are introduced into the gap regime and moving towards the Dirac point symmetrically. They correspond to n- and p-type channels, respectively. In order to elucidate this behavior, we calculate the eigenstates and eigenenergies of the isolated GNRs with configurations employed in Fig. 2(a) and the results are plotted in Fig. 3(a). The eigenenergies are indicated by points with the same color

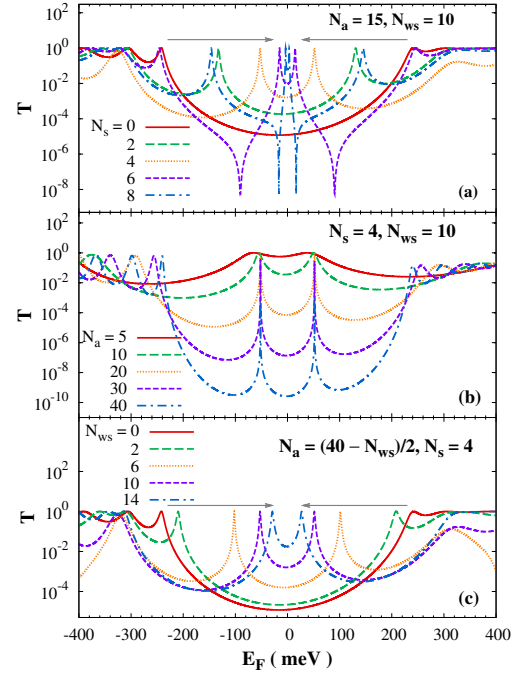


FIG. 2: (Color online) Transmission  $T$  as function of the Fermi energy of in the GNR with one sidearm shown in Fig. 1: (a) dependence on the length of the sidearm  $N_s$ . The two gray arrows here and hereafter are plotted to indicate the evolution of quantities with the varying of parameters, accordingly; (b) dependence on the total length of the GNR  $N_a$ ; (c) dependence on the width of the sidearm  $N_{ws}$ . All necessary parameters are indicated in the corresponding figures.

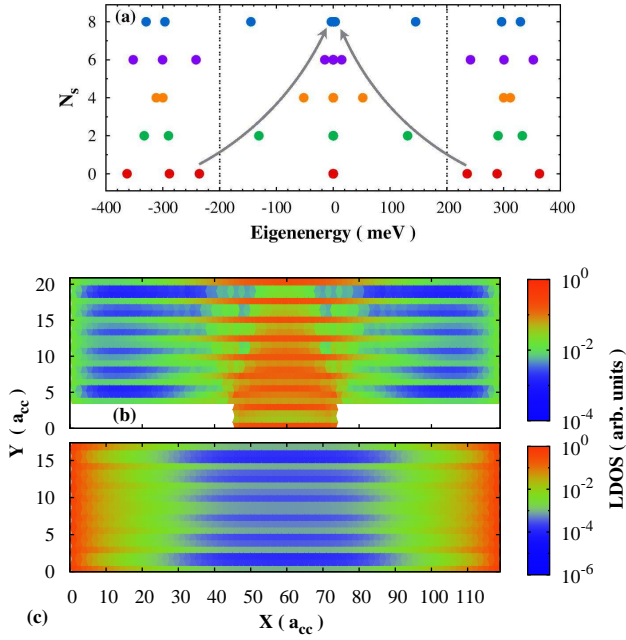


FIG. 3: (Color online) (a) Eigenenergies in the isolated GNR with configurations being the same as those in Fig. 2(a). The gap regime is indicated between the two dashed lines. Local density of states in the GNR at Fermi energy  $E_F = 51.511$  meV: (b) corresponding to the right peak in the gap shown in Fig. 2(b) for  $N_a = 15$ ,  $N_{ws} = 10$  and  $N_s = 4$ ; and (c) in the same condition but without a sidearm.  $a_{cc}$  is the carbon-carbon bond distance. Note that the scale in the  $y$ -axis is elongated to make the figures clearer and the local density of states in the leads are not included.

as in Fig. 2(a) for the corresponding length of the sidearm  $N_s$ . It is noted that the states with eigenenergies at the Dirac point are the localized edge states in the zigzag terminals,<sup>11–13</sup> which do not really exist when the terminals are connected to the metal leads. Apart from these fake states, as indicated by the gray arrows, two states (even more for  $N_s \geq 8$ ) come into the gap and move towards the Dirac point symmetrically. By comparing Fig. 2(a) and Fig. 3(a), close correspondence between the positions of the conduction peaks and those of the eigenenergies is seen. We hence conclude that the transport behavior in this structure of a small size can be understood as resonant tunneling through the GNR via the confined states therein. We then examine how the conduction peaks induced by the sidearm are influenced by the total length of the GNR. From Fig. 2(b), one observes that the positions of conduction peaks are insensitive to the total length of the GNR. This suggests that the states which contribute to the conduction peaks distribute mainly in the sidearm region. Moreover, with the increase of the total length of the GNR, the confined states are less coupled to the leads. As a result, the conduction peaks are narrowed and the transmissions in the gap regime other than the conduction peaks are suppressed. In addition, as shown in Fig. 2(c), a wider

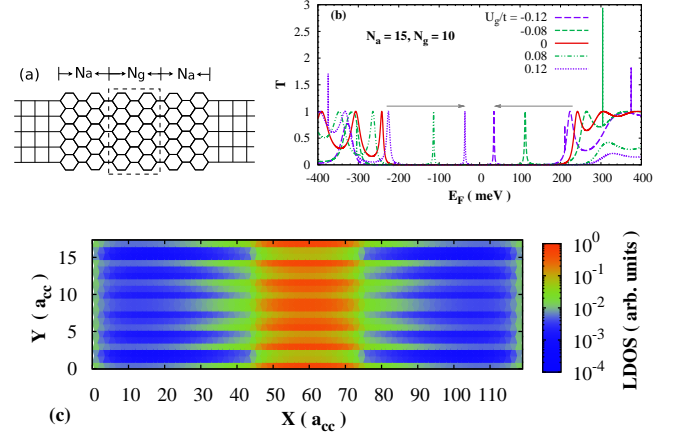


FIG. 4: (Color online) (a) Schematic view of the armchair GNR with on-site gate voltage deposited in the region labelled with dashed box. (b) Transmission  $T$  as function of the Fermi energy of in the GNR with a gate voltage shown in (a), for different values of on-site energy  $U_g$ . (c) Local density of states in the GNR corresponding to the conduction peak induced by an on-site gate voltage  $U_g = -0.12t$  in (b), at Fermi energy  $E_F = 33.405$  meV. All necessary parameters are indicated in the corresponding figures.

sidearm is more effective in bringing conduction peaks into the gap regime.

It is illustrative to perform a spatial analysis of the conductance. In Fig. 3(b), we plot the local density of states in the GNR corresponding to the right conduction peak shown in Fig. 2(b) for  $E_F = 51.511$  meV,  $N_a = 15$ ,  $N_{ws} = 10$  and  $N_s = 4$ ; and in Fig. 3(c) for the same condition but without the sidearm. One observes that distinct from the case without the sidearm where the electronic state is restricted in the vicinities of the two terminals, the state contributing to the conduction peak indeed mostly distributes in the sidearm region. This kind of bound states have been discussed by Sevinçli *et al.*<sup>30</sup> and Prezzi *et al.*<sup>31</sup> in the superlattice structures of GNR. The underlying physics is that, since the energy band gap of armchair GNR shows strong dependence on the ribbon width, one can fabricate structures similar to the conventional semiconductor heterojunctions by joining GNRs with different widths. In the condition shown in Fig. 3(b), segments of armchair GNRs with widths  $M = 21, 25$  and  $21$  are joined together. The band gaps of the corresponding infinite GNRs with the same widths are  $(-200, 200)$ ,  $(-140, 140)$  and  $(-200, 200)$  meV, respectively. Therefore, the GNR with one sidearm resembles the quantum well structure in semiconductors with conduction- and valence-band offset  $\Delta = 60$  meV, and hence the bound states are formed therein. It is further noted that due to the finite lengths of the GNR segments and the detailed joining condition, the actual band offset is different from the above simple estimation.

Following the idea of introducing bound states into the gap regime, we then propose another way of access-

ing states inside the band gap by using an on-site gate voltage.<sup>32,33</sup> As illustrated in Fig. 4(a), we apply a positive (negative) voltage in the framed region by a top gate<sup>22</sup> which acts as a well potential to electrons (holes). The transmissions as function of the Fermi energy are plotted in Fig. 4(b) for different values of the gate voltage. One observes that by increasing the strength of positive (negative) gate voltage, a conduction peak enters the gap regime from the right (left) and moves towards the left (right). These conduction peaks are from the tunneling via the bound states in the gapped region.<sup>32</sup> We

demonstrate this by plotting the local density of states in Fig. 4(c), which corresponds to the conduction peak induced by a gate voltage  $U_g = -0.12t$ . In the sense that here one can introduce only one conduction peak into gap regime with its position fully determined by the gate voltage, this configuration has the advantage to serve as an energy filter. The influences of the width of the gate region and the total length of the GNR on the induced conduction peaks resemble the case with one sidearm, and are not explicitly plotted.

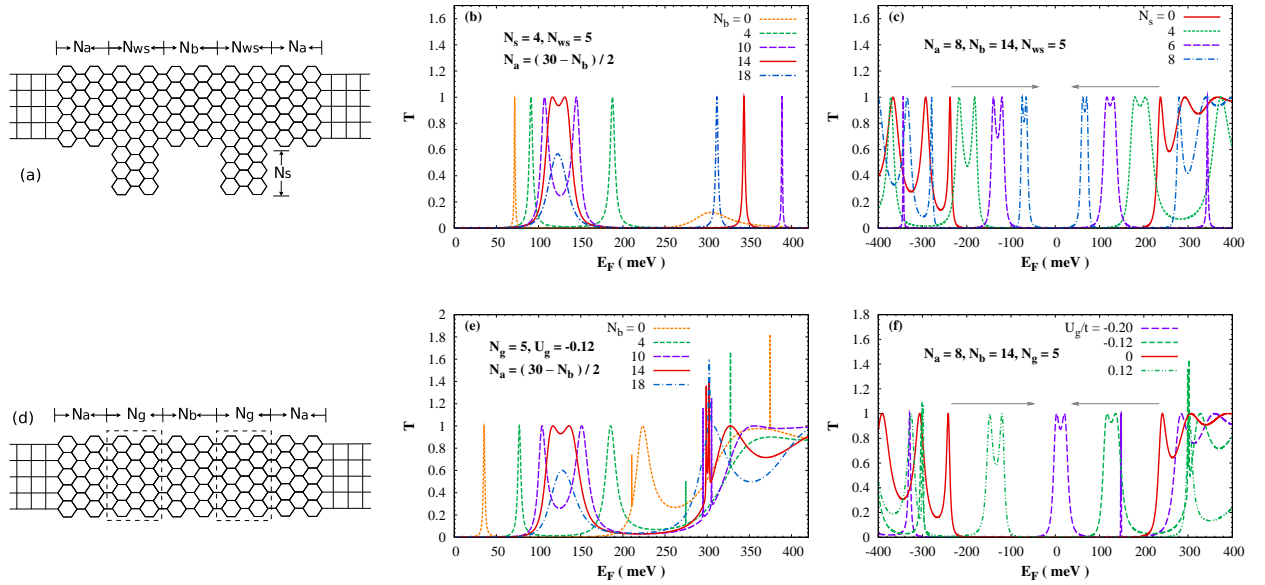


FIG. 5: (Color online) (a) and (d) Schematic view of the armchair GNR with two sidearms and two on-site gates, respectively. Transmission  $T$  as function of the Fermi energy in the GNR shown in (a): (b) dependence on the spacing between the two sidearms  $N_b$ ; (c) dependence on the length of the sidearms  $N_s$ . Transmission  $T$  as function of the Fermi energy in the GNR shown in (d): (e) dependence on the spacing between the two gates  $N_b$ ; (f) dependence on the values of on-site energy  $U_g$  induced by the gate voltage. All necessary parameters are indicated in the corresponding figures.

### B. Electronic transport in GNRs with two sidearms or on-site gate voltages

Due to the fact that the conduction peaks introduced into the gap regime are extremely sharp in the above two configurations and hence are easily destroyed by disorders as we will show below, we further propose two schemes of structures to improve the robustness, i.e., by employing two sidearms or gate voltages shown in Fig. 5(a) and (d).<sup>26,34–36</sup> It is noted that here we fix the total length of the GNRs  $N_{\text{tot}} = 40$  and the total width of the two sidearms or the gates is set to be the same width of the sidearm or gate region in the previous configurations. In searching for the best performance of the devices, i.e., a wide conduction window, we vary the spacing length

$N_b$  between the two sidearms or gate regions to modify the interference between tunnelings via the two (quasi-)bound states from the dual structure. The results are plotted in Fig. 5(b) and (e), for the situations with two sidearms and two gates, respectively. It is found that for both cases with  $N_b = 14$ , a conduction plateau is formed with a wide energy window up to 50 meV centered around  $E_F = 125$  meV (red solid curves in the figure). Such a wide conduction window in the original gate region allows a large current in the “on” state of the proposed device which is of potential use for high performance field-effect transistors. Moreover, as shown in Fig. 5(c) and (f), the positions of the conduction plateaus can be controlled by the length of the sidearms and by on-site gate voltage, respectively. So the excellent feature of controlled modi-

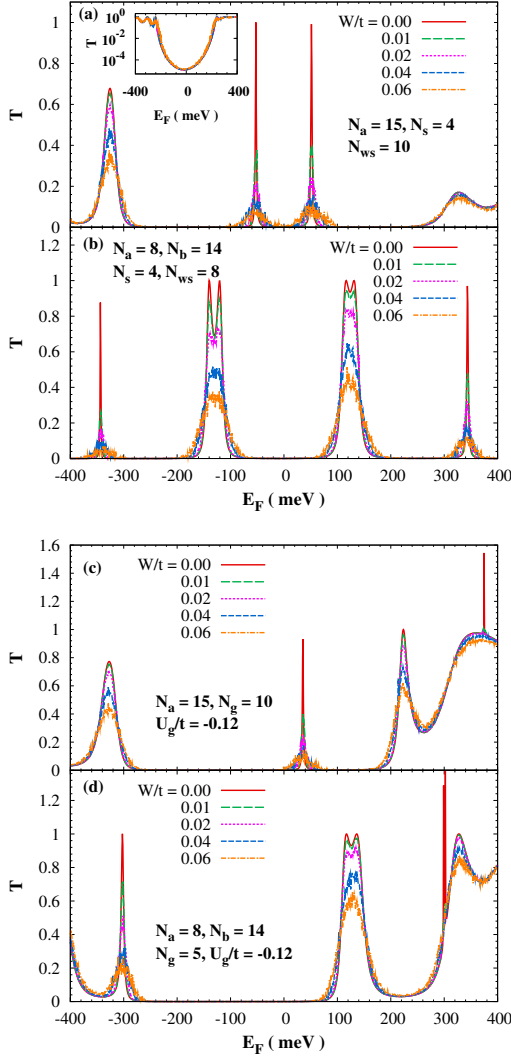


FIG. 6: (Color online) Transmission  $T$  as function of the Fermi energy with different Anderson disorder strength  $W$  in the GNR: (a) and (b) with one and two sidearms [corresponding to GNR structures shown in Fig. 1 and Fig. 5(a)], respectively; (c) and (d) with one and two one-site gate voltages [corresponding to GNR structures shown in Fig. 4(a) and Fig. 5(d)], respectively. All necessary parameters are indicated in the corresponding figures.

figuration of the conduction window is preserved in the dual structures.

### C. Disorder analysis

We now show the feasibility of the above proposed devices for real application by analyzing the robustness of the switch-off character, and more importantly the conduction peaks and plateaus against the Anderson disorder.<sup>20,26</sup> In our simulation, the Anderson disorder is created out by introducing random on-site energy at

the carbon atoms:  $\varepsilon'_{i_c} = \varepsilon_{i_c} + \lambda W$  [see Eq. (3)]. Here  $W$  is the disorder strength and  $\lambda$  is a random number with a uniform probability distribution in the range  $(-1, 1)$ . The converged transmissions are obtained by averaging over 100 random configurations.<sup>26</sup> The results of pristine GNR without a sidearm or on-site gate voltage are plotted in the inset of Fig. 6(a). One notices that under different strength of disorder, all five curves almost coincide with each other. This indicates that the gap behavior is very robust against disorder, which ensures extremely small leakage current in the “off” state of the device. We then turn to check the robustness of the “on” state of the proposed structures. By comparing the corresponding curves in Fig. 6(a) and (b), one finds that the conduction peaks from one sidearm rapidly decrease with the strength of the disorder whereas the conduction plateaus from two sidearms are more sustained. The latter are only reduced by about 50% for the largest disorder strength  $W = 0.06t$ . Therefore, the robustness is immensely improved by using two sidearms to introduce a wide conduction window into the gap regime. The situation for configurations with one or two gate voltages is similar. So we only plot our results in Fig. 6(c) and (d) without more discussions. In this way, we demonstrate the robustness of the proposed devices for both “on” and “off” states.

## IV. SUMMARY

In summary, we have proposed two schemes for field-effect transistor, which may also work as energy filter, by studying transport properties in the GNR-based structures with sidearms or on-site gate voltages. Gapped armchair GNRs are employed with the band gap used as a natural “off” state of the transistor. Metal leads are employed so that by further introducing a sidearm or on-site gate voltage to the GNR, one is able to access the gap regime with conduction peaks. Moreover, by employing two sidearms or on-site gate voltages, we obtain much wider conduction windows with the transmission close to one, which allows a large “on” current. We show that the positions of the conduction peaks or plateaus can be controlled by the length of the sidearm (which can be modulated by a gate voltage), or by the voltage of the on-site gates on the GNR. This property enables the proposed devices not only serve as a common transistor with large on/off ratio, but also as an energy filter. We further demonstrate the robustness of both the “off” and “on” states of the devices against disorder. The excellent switch-off ability, the wide conduction window of “on” state which allows controlled modifications and the high robustness against disorder suggest that the proposed structures have great potential to work as high performance field-effect transistor in reality.

## Acknowledgments

This work was supported by the National Basic Research Program of China under Grant No.

2012CB922002 and the National Natural Science Foundation of China under Grant No. 10725417.

- 
- \* Electronic address: mwwu@ustc.edu.cn.
- <sup>1</sup> K. S. Novoselov, A. K. Geim, S. V. Morozov, D. Jiang, Y. Zhang, S. V. Dubonos, I. V. Grigorieva, and A. A. Firsov, *Science* **306**, 666 (2004).
  - <sup>2</sup> A. K. Geim and K. S. Novoselov, *Nature Mater.* **6**, 183 (2007); A. K. Geim, *Science* **324**, 1530 (2009); A. H. Castro Neto, F. Guinea, N. M. R. Peres, K. S. Novoselov and A. K. Geim, *Rev. Mod. Phys.* **81**, 109 (2009).
  - <sup>3</sup> S. Das Sarma, S. Adam, E. H. Hwang, and E. Rossi, *Rev. Mod. Phys.* **83**, 407 (2011).
  - <sup>4</sup> M. Y. Han, B. Özyilmaz, Y. Zhang, and P. Kim, *Phys. Rev. Lett.* **98**, 206805 (2007).
  - <sup>5</sup> M. Y. Han, J. C. Brant, and P. Kim, *Phys. Rev. Lett.* **104**, 056801 (2010).
  - <sup>6</sup> X. Li, X. Wang, L. Zhang, S. Lee, and H. Dai, *Science* **319**, 1229 (2008).
  - <sup>7</sup> J. Cai, P. Ruffieux, R. Jaafar, M. Bieri, T. Braun, S. Blankenburg, M. Muoth, A. P. Seitsonen, M. Saleh, X. Feng, K. Müllen, and R. Fasel, *Nature* **466**, 470 (2010).
  - <sup>8</sup> L. Jiao, L. Zhang, X. Wang, G. Diankov, and H. Dai, *Nature* **458**, 877 (2009).
  - <sup>9</sup> D. V. Kosynkin, A. L. Higginbotham, A. Sinitskii, J. R. Lomeda, A. Dimiev, B. K. Price, and J. M. Tour, *Nature* **458**, 872 (2009).
  - <sup>10</sup> F. Schwierz, *Nature Nanotech.* **5**, 487 (2010).
  - <sup>11</sup> M. Fujita, K. Wakabayashi, K. Nakada, and K. Kusakabe, *J. Phys. Soc. Jpn.* **65**, 1920 (1996).
  - <sup>12</sup> K. Nakada, M. Fujita, G. Dresselhaus, and M. S. Dresselhaus, *Phys. Rev. B* **54**, 17954 (1996).
  - <sup>13</sup> K. Wakabayashi, M. Fujita, H. Ajiki, and M. Sigrist, *Phys. Rev. B* **59**, 8271 (1999).
  - <sup>14</sup> X. Wang, Y. Ouyang, X. Li, H. Wang, J. Guo, and H. Dai, *Phys. Rev. Lett.* **100**, 206803 (2008).
  - <sup>15</sup> D. A. Areshkin, D. Gunlycke, and C. T. White, *Nano Lett.* **7**, 204 (2007).
  - <sup>16</sup> V. H. Nguyen, V. N. Do, A. Bournel, V. L. Nguyen, and P. Dollfus, *J. Appl. Phys.* **106**, 053710 (2009).
  - <sup>17</sup> J. W. González, M. Pacheco, L. Rosales, and P. A. Orellana, *Phys. Rev. B* **83**, 155450 (2011).
  - <sup>18</sup> K. Saloriotta, Y. Hancock, A. Kärkkäinen, L. Kärkkäinen, M. J. Puska, and A.-P. Jauho, *Phys. Rev. B* **83**, 205125 (2011).
  - <sup>19</sup> A. Lherbier, B. Biel, Y.-M. Niquet, and S. Roche, *Phys. Rev. Lett.* **100**, 036803 (2008).
  - <sup>20</sup> G. Schubert, J. Schleede, and H. Fehske, *Phys. Rev. B* **79**, 235116 (2009).
  - <sup>21</sup> E. R. Mucciolo, A. H. Castro Neto, and C. H. Lewenkopf, *Phys. Rev. B* **79**, 075407 (2009).
  - <sup>22</sup> L. Liao, J. W. Bai, R. Cheng, Y.-C. Lin, S. Jiang, Y. Huang, and X. F. Duan, *Nano Lett.* **10**, 1917 (2010).
  - <sup>23</sup> J. P. Robinson and H. Schomerus, *Phys. Rev. B* **76**, 115430 (2007).
  - <sup>24</sup> Ya. M. Blanter and I. Martin, *Phys. Rev. B* **76**, 155433 (2007).
  - <sup>25</sup> B. Huard, J. A. Sulpizio, N. Stander, K. Todd, B. Yang, and D. Goldhaber-Gordon, *Phys. Rev. Lett.* **98**, 236803 (2007).
  - <sup>26</sup> K. Shen and M. W. Wu, *Phys. Rev. B* **77**, 193305 (2008).
  - <sup>27</sup> As shown in Ref. 16, a change in the ratio  $t_\alpha/t$  or in the value of  $t_T$  does not qualitatively affect the overall features of transport. Here we take  $t_\alpha = t_T = t$ , corresponding the case with ballistic tunneling in the GNR-lead interface.<sup>23,24</sup>
  - <sup>28</sup> M. Büttiker, *Phys. Rev. Lett.* **57**, 1761 (1986).
  - <sup>29</sup> S. Datta, *Electronic Transport in Mesoscopic Systems* (Cambridge University Press, New York, 1995).
  - <sup>30</sup> H. Sevinçli, M. Topsakal, and S. Ciraci, *Phys. Rev. B* **78**, 245402 (2008).
  - <sup>31</sup> D. Prezzi, D. Varsano, A. Ruini, and E. Molinari, *Phys. Rev. B* **84**, 041401 (2011).
  - <sup>32</sup> P. G. Silvestrov and K. B. Efetov, *Phys. Rev. Lett.* **98**, 016802 (2007).
  - <sup>33</sup> P. Recher and J. Nilsson, G. Burkard, and B. Trauzettel, *Phys. Rev. B* **79**, 085407 (2009).
  - <sup>34</sup> M. Barbier, F. M. Peeters, P. Vasilopoulos, and J. M. Pereira, *Phys. Rev. B* **77**, 115446 (2008).
  - <sup>35</sup> L. Wang, K. Shen, S. Y. Cho, and M. W. Wu, *J. Appl. Phys.* **104**, 123709 (2008).
  - <sup>36</sup> Y. P. Bliokh, V. Freilikher, S. Savel'ev, and F. Nori, *Phys. Rev. B* **79**, 075123 (2009).